JIMA Vol. 74, No. 2 (June 2022) pp. 47-59.

Original

Effect of lumbar anterior longitudinal ligament rupture on initial instrument fixation: a three-dimensional finite element method study

Hirotaka YAN, Hirooki ENDO,
Daisuke YAMABE, Yusuke CHIBA, Ryosuke OIKAWA,
Hideki MURAKAMI and Minoru DOITA

Department of Orthopedic Surgery, School of Medicine,
Iwate Medical University, Yahaba, Japan

(Received on December 28, 2021 & Accepted on February 5, 2022)

Abstract

Recent studies on adult spinal deformity report complications including anterior longitudinal ligament (ALL) rupture, which may cause instrumentation failure. This study aimed to evaluate the effect of ALL rupture on instrumentation failure. We used a three-dimensional finite element method (3D-FEM) to study the rupture of the ALL. A 3D-FEM model of the lumbar spine was generated using computed tomography images. A posterior instrument was then adapted to the L1-S1 vertebrae as a fixed model. Simulations of ALL rupture were performed at L3/4 in 25% increments and virtual excision of the intervertebral disc (IVD) was performed for each model. Thus, we prepared standard models and L1-S1 fixed models with and without disc excision under ALL rupture conditions. We evaluated displacement (mm) during extension and the von Mises stress (MPa) on the IVD, vertebral body around the screws, and posterior instrument. In the standard models, with and without disc excision, displacement during extension and the stress on IVDs increased as the degree of ALL rupture increased. In L1-S1 fixed models, the displacement similarly increased. The stress on IVDs, vertebral bodies around the screws, and posterior instruments also increased. ALL rupture may pose a potential risk of vertebral instability, leading to instrumentation failure.

Key words : *anterior longitudinal ligament rupture, instrumentation failure, three-dimensional finite element method, adult spinal deformity, lateral lumbar interbody fusion*

I. Introduction

Adult spinal deformity (ASD), a common condition associated with low health-related quality-of-life outcomes, is increasing in prevalence and reportedly affects up to 68% of elderly people [1-3]. Although we usually prescribe conservative treatment for patients with mild or moderate symptoms, surgery is often necessary for patients with severe symptoms, such as low back pain and/or gait disturbance caused by spinal malalignment. In most cases, surgery for restoration of spinal malalignment improves the quality of life of

Corresponding author: Hirooki Endo
oki_oki@me.com

patients. With this aim in mind, it is better to choose a procedure that is as minimally invasive as possible because patients with ASD are often of advanced age and cannot tolerate invasive procedures [4]. This explains why in recent times, good results have been reported for minimally invasive multilevel lateral lumbar interbody fusion (LLIF), including extreme lateral lumbar interbody fusion and oblique lateral lumbar interbody fusion, with posterior instrumented fixation for the correction of spinal deformities in elderly patients [5–14].

Several studies on ASD have also reported frequent mechanical complications, including rod fracture, screw breakage or loosening, interbody spacer migration, and hook dislodgment [15–19]. In addition, anterior longitudinal ligament (ALL) rupture is a known intraoperative complication of LLIF [20–22] that causes vertebral instability and potentially leads to instrumentation failure followed by delayed union and pseudoarthrosis [23–26]. One Japanese observational study found that ALL rupture occurred in 14 out of 34 patients (41.2%) with ASD who underwent LLIF, and delayed union was indicated in this group [26]. However, there are no reports in the literature that focus on ALL rupture, which can influence posterior instrumentation and cause mechanical complications. We hypothesized that stress on the tissues and posterior instrument would increase as the degree of ALL rupture increased. The present study aimed to investigate the association between ALL rupture and instrumentation failure, using a three-dimensional finite element method (3D-FEM).

II. Materials and Methods

1. Finite element model of the lumbar vertebrae with posterior instrumentation

A 3D-FEM lumbar model consisting of the five vertebral bodies, sacrum, ALL, posterior longitudinal ligament, ligamentum flavum, and intervertebral disc (IVD), was created using helical computed tomography (CT) images (0.6 mm slice thickness) of the whole spine, from the cervical spine to the pelvis, of a healthy adult woman with a dual source CT scanner (SOMATOM Force; Siemens Healthineers AG, Erlangen, Germany). The scanning parameters were as follows: field of view (FOV) = 330 mm; tube voltage = 90 kV; tube current with CT-automatic exposure control (CT-AEC) = 200 reference mAs; rotation time = 0.5 s/rot. Image series were reconstructed by using advanced modeled iterative reconstruction (ADMIRE). The vertebral body was differentiated into cortical and cancellous bones, based on actual CT scan measurements, so that the thickness of the cortical shell had a range of between 1.5 and 2.0 mm and the IVD included the annulus fibrosus and the nucleus pulposus. We used Simpleware Scan IP Version N-2018.3 (Synopsys, Inc., Mountain View, CA, USA) for analysis and spatial resolution of the CT scan was not modified when transferring data. In addition, L1-S1 screws and rods were optimally fabricated using Simpleware Scan IP (Synopsys, Inc.) and Inventor 2019 (Autodesk, Inc., Mill Valley, CA, USA). Thus, the standard model and the L1-S1 fixed model were completed. These models were divided into all 4-node tetrahedral elements (Fig. 1A).

Table 1. Material properties of the present model

	Young modulus (MPa)	Poisson ratio
Cortical bone	12,000	0.30
Cancellous bone	1,500	0.30
Annulus fibrosus	25	0.30
Nucleus pulposus	1	0.45
Anterior longitudinal ligament	68	0.30
Posterior longitudinal ligament	98	0.30
Ligamentum flavum	28.6	0.30
Titanium alloy	110,000	0.30

2. Material properties and boundary conditions

We imported all meshed parts of the lumbar model, including the posterior instrument, from the initial software to the secondary software, Patran 2008r2 Pre Release (MSC Software, Inc., Newport Beach, CA, USA), as pre-post processors. These parts were assigned for complete adhesion under node sharing with each other except for each facet joint, as suggested in previous studies [27, 28], and the posterior instruments of the L1-S1 fixed model were assumed to be firmly inserted and fixed into the bone. After node sharing, the standard model had 226,906 nodal points and 1,093,629 elements in total, and the L1-S1 fixed model had 310,909 nodal points and 1,499,182 elements in total. The material properties of the anatomical components were set with reference to earlier studies, and titanium alloy (Ti-6Al-4V) was the material chosen for the instruments (Table 1) [29–32]. These properties included Young modulus and Poisson ratio, which meant a measure of stiffness of an elastic material and the ratio of transverse contraction strain to longitudinal extension strain in the direction of stretching force, respectively. The caudal part of the sacrum was fixed in all directions to simulate a constraint condition. Loads of 500 N were applied to the cephalic margins of L1, upward in the anterior margin and downward in the posterior margin. These conditions were defined as static load conditions to recreate lumbar extension. This boundary condition did not have "the follower load" cited in previous 3D-FEM studies, considering the physiological compressive load caused by muscle contraction [33–35]. This approach was taken because the present study aimed to evaluate only the influence of ALL rupture.

3. Simulation of ALL rupture and disc excision during surgery

We hypothesized that ALL rupture would occur in either one or both anterior approaches, such as the LLIF and posterior cantilever technique, so the ALL at L3/4 in each model was differentiated by 25% increments (0%, 25%, 50%, 75%, and 100% of ALL rupture) using Patran 2008r2 Pre Release (MSC Software, Inc.) (Fig. 1B). The L3/4 level was empirically selected because there have

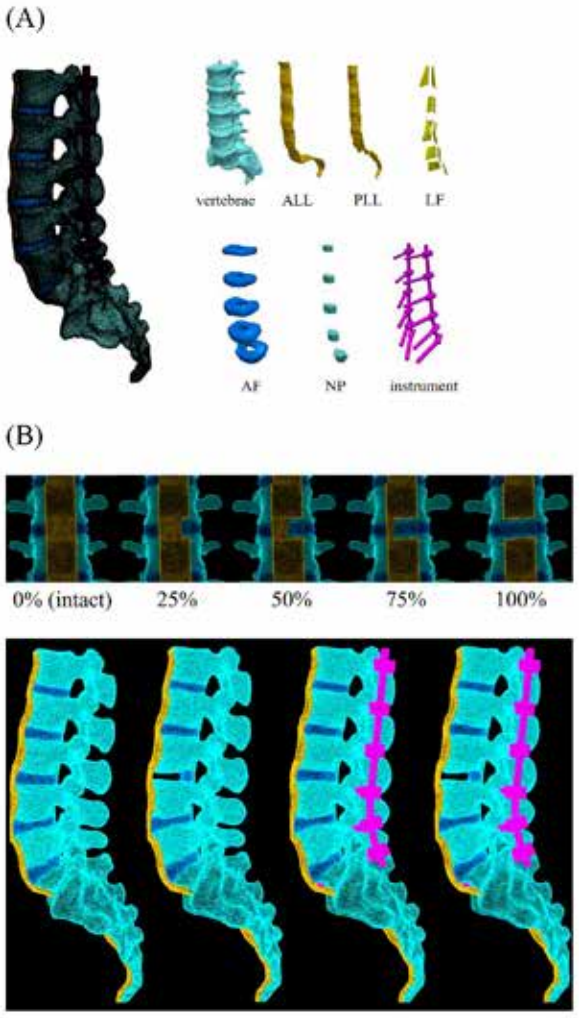

Fig. 1. A three-dimensional finite element lumbar model (A) and preparation for analysis (B).
(A) This model consists of the five vertebral bodies, sacrum, anterior longitudinal ligament (ALL), posterior longitudinal ligament (PLL), ligamentum flavum (LF), annulus fibrosus (AF), nucleus pulposus (NP), and posterior instrument.
(B) Simulation of anterior longitudinal ligament rupture at L3/4 in 25% increments (upper). The standard models and the L1-S1 fixed models with or without disc excision (lower).

IVD around the screws and the posterior instrument, using Marc 2010 (MSC Software, Inc.) as the solver. We did not consider the values at L1/2 and L5/S1 because we could not evaluate the stress accurately owing to

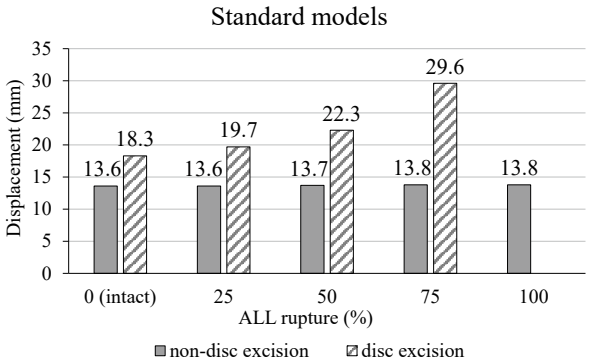

Fig. 2. Displacement in the standard models.
The standard models with and without disc excision are physiologically extended with an increase in the degree of anterior longitudinal ligament (ALL) rupture. Displacement during extension in the models with or without disc excision increases as the degree of ALL rupture increases. In models with disc excision, the spinous processes of the 75% ALL rupture model impinged on one another at L3/4 and analytic errors in the 100% ALL rupture model provided no data.

the analytically and structurally inevitable stresses at those levels in our study conditions. Moreover, the finite element method, which is different from statistics, is one of the methods of numerical analysis and is used to find approximate solutions to differential equations. This method is deeply rooted in functional analysis and mathematically well-ordered. Marc 2010 (MSC Software, Inc.) performs analyses based on this theory, so a statistical approach was unnecessary in the present study.

III. Results

Figure 2 shows the displacement during extension in the standard models with and without disc excision. The displacement in models without and with disc excision increased from 13.6 mm to 13.8 mm and

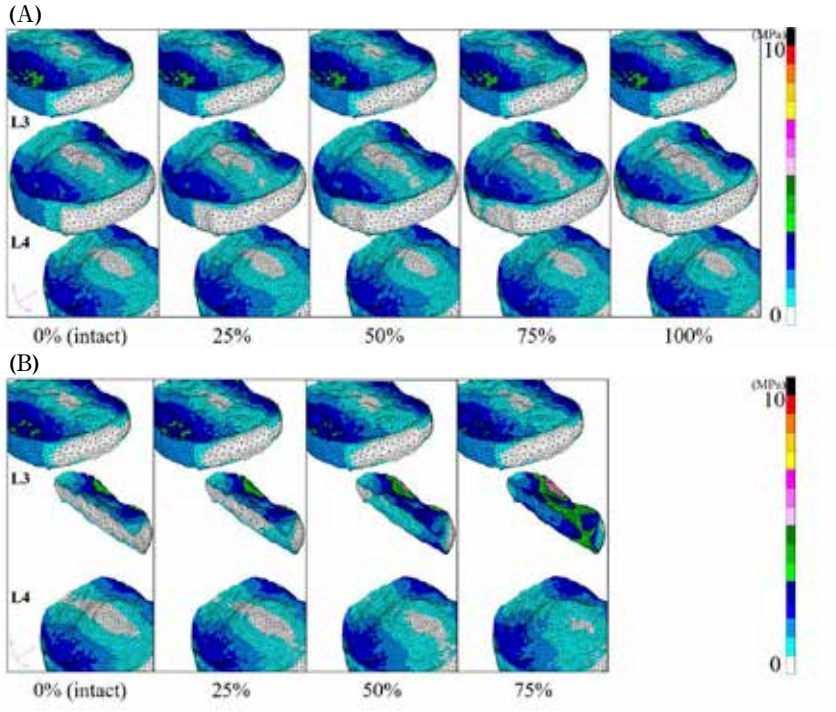

Fig. 3. Stress distribution of the intervertebral disc in the standard models.
(A) A case without disc excision, where the stress is expressed as von Mises stress (MPa) using the contour map and increases as the degree of anterior longitudinal ligament (ALL) rupture increases.
(B) A case with disc excision (lower), where the stress is expressed as von Mises stress (MPa) using the contour map and increases as the degree of ALL rupture increases. Analytic errors in the 100% ALL rupture model provide no data.

from 18.3 mm to 29.6 mm, respectively, as the degree of ALL rupture increased. In the models with disc excision, the spinous processes in the 75% ALL rupture model impinged on one another at L3/4, and analytic errors in the 100% ALL rupture model provided no data. The upper panel of Figure 3 demonstrates the stress distribution of the IVD in the standard models without disc excision. The anterior stress of the IVD at L3/4 decreased from 0.667 MPa to 3.33 MPa, and the posterior stress increased from 0.667 MPa to 4.00 MPa as the degree of ALL rupture increased. The lower panel of Figure 3 demonstrates the stress distribution of the IVD in the standard models with disc excision.

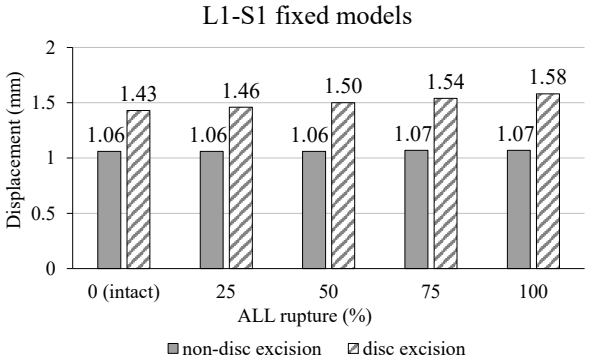

Fig. 4. Displacement in the L1-S1 fixed models.
Displacement during extension in the models with or without disc excision increases as the degree of anterior longitudinal ligament rupture increases.

The stress of the residual IVD at L3/4 and the whole stress of the IVD at L4/5 increased from 0.667 MPa to 8.67 MPa and from 0.667

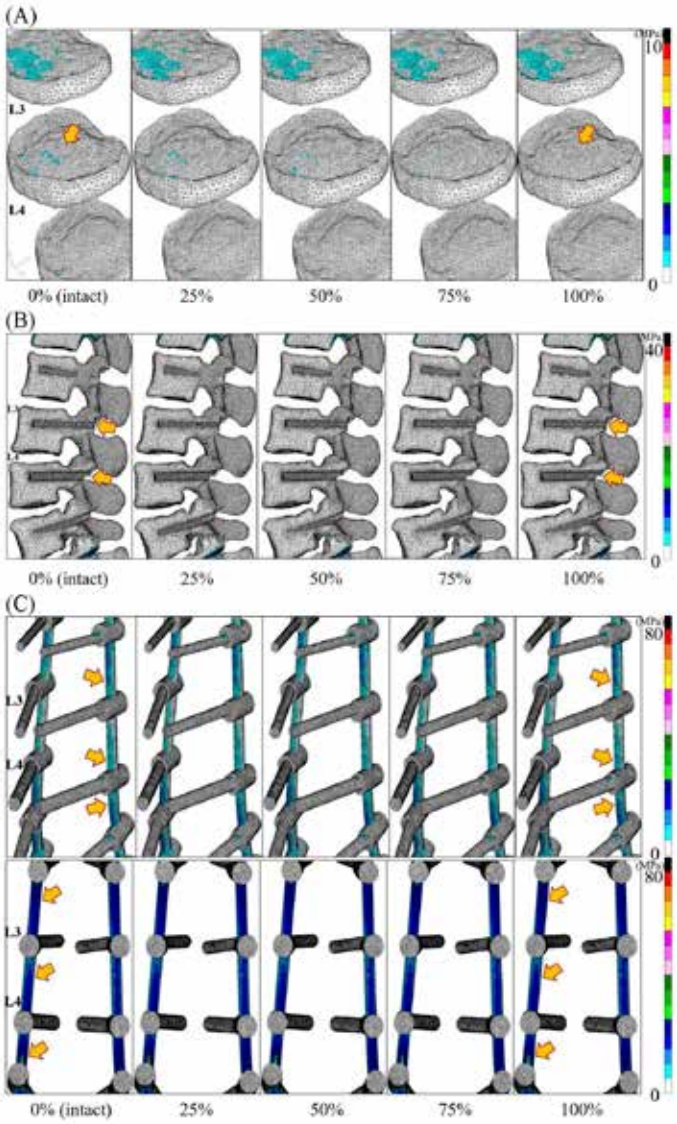

Fig. 5. Stress distribution in the L1-S1 fixed models without disc excision.
Stress is expressed as von Mises stress (MPa) using the contour map. The stress of the anterior part of the intervertebral disc (A) decreases and increases in the posterior part. The stress of the vertebral bodies around the screws (B) and the posterior instruments (C) increases as the degree of anterior longitudinal ligament (ALL) rupture increases. The arrows of intact and 100% show the easy-to-understand locations where stress distribution can change in each part among the degree of ALL rupture.

MPa to 3.33 MPa, respectively, as the degree of ALL rupture increased. In excised cases, analytic errors in the 100% ALL rupture model provided no data.

Figure 4 shows the displacement during extension in the L1-S1 fixed models, with and without disc excision. The displacement in models without and with disc excision increased from 1.06 mm to 1.07 mm and from 1.43 mm to 1.58 mm, respectively, as the degree of ALL rupture increased. Figure 5 demonstrates the stress distribution of the IVD, the vertebral bodies around the screws, and the posterior instruments in the L1-S1

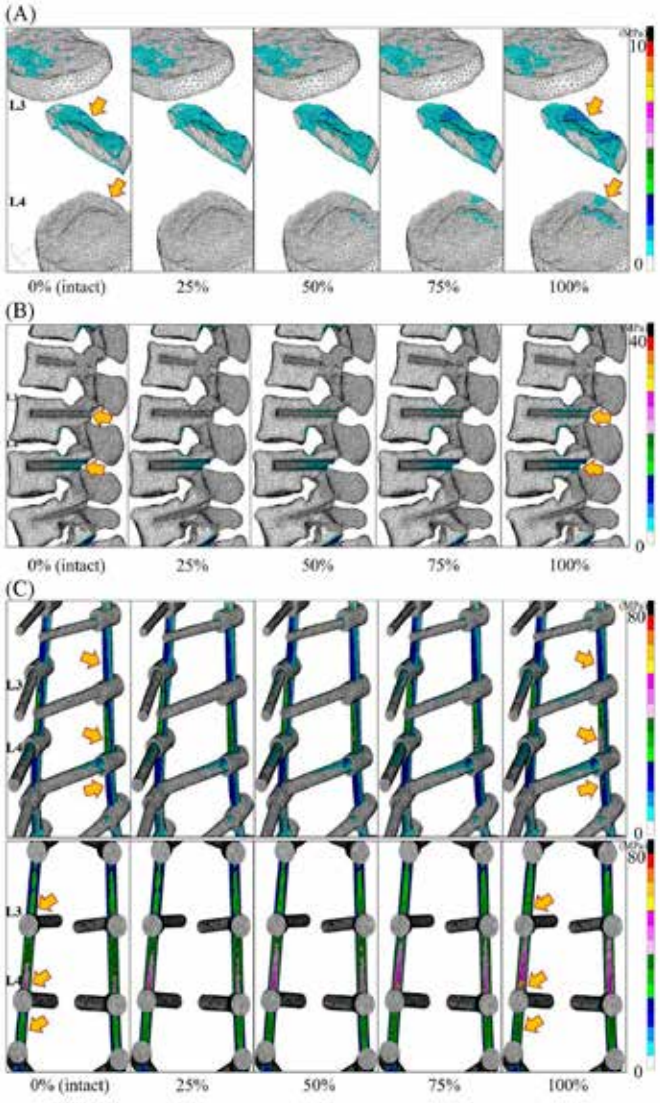

Fig. 6. Stress distribution in the L1-S1 fixed models with disc excision.
Stress is expressed as von Mises stress (MPa) using the contour map. The stress of the intervertebral disc (A) , the vertebral bodies around the screws (B), and the posterior instruments (C) increase as the degree of anterior longitudinal ligament (ALL) rupture increases. The arrows of intact and 100% show the easy-to-understand locations where stress distribution can change in each part among the degree of ALL rupture.

fixed models without disc excision. The overall stress of the IVD at L2/3, L3/4, and L4/5 decreased more than that in the standard models (Fig. 3A). The anterior stress of the IVD at L3/4 decreased from 0.290 MPa to 0.865 MPa, and the posterior stress increased from 0.147 MPa to 0.577 MPa as the degree of ALL rupture increased. The stress of the vertebral bodies around the screws at L3 and L4 increased from 0.732 MPa to 2.20 MPa and from 0.732 MPa to 2.93 MPa, respectively, as the degree of ALL rupture increased. The stress of the posterior instruments at L2/3, L3/4, and L4/5 increased from 5.33 MPa to 32.0 MPa each as the degree of ALL rupture increased. Figure 6 demonstrates the

stress distribution of the IVD, the vertebral bodies around the screws, and the posterior instruments in the L1-S1 fixed models with disc excision. The overall stress of the IVD at L2/3, L3/4, and L4/5 decreased more than that in the standard models (Fig. 3B). The stress of the residual IVD at L3/4 and the posterior stress of the IVD at L4/5 increased from 0.667 MPa to 2.00 MPa and from 0.667 MPa to 1.33 MPa, respectively, as the degree of ALL rupture increased. The stress of the vertebral bodies around the screws at L3 and L4 increased from 2.67 MPa to 8.00 MPa and from 2.67 MPa to 13.3 MPa, respectively, as the degree of ALL rupture increased. The stress of the posterior instruments at L2/3, L3/4, and L4/5 increased from 5.33 MPa to 80.0 MPa each as the degree of ALL rupture increased.

IV. Discussion

The stress distribution in our intact standard model without disc excision (ALL 0% rupture) showed that the anterior parts of the IVDs were pulled by the vertebral bodies, and the posterior parts were compressed. At the same time, there were neutral zones almost in the center of the IVDs. This result could demonstrate the path approximating the tangent to the curvature of the lumbar vertebrae in a similar fashion to that reported in the literature using "the follower load" [33–35]. Both the stress and displacement of the intact standard model increased more with excision, and this result could explain why the IVD was an anterior retainer construction as well as ALL. Considering these points, the physiological extension and the realistic lumbar construct in the present study model were validated. We showed that the displacement during extension and the stress on the IVDs, vertebral bodies around the screws, and posterior instruments (both screws and rods) increased as the degree of ALL rupture increased.

It is generally known that ALL tethers each vertebral body and suppresses bulging of the IVD, thereby retaining extension and axial rotation [36]. Based on this characteristic of ALL, previous studies have investigated the influence of ALL rupture using a variety of methods. Some studies have found that the excision of ALL caused hypermobility at the excision level and adjacent levels [37, 38]. A prospective study on total disc replacement suggested that the maintenance of ALL led to evasion of instrumentation failure and good alignment by ligamentotaxis [39]. A pathological study on rabbits found that injury to the IVD accompanied by complete ALL rupture caused spinal instability [40]. Furthermore, an earlier cadaveric study demonstrated that ALL excision led to significant instability of constructs and potential risk of instrumentation failure, even if those constructs had 8 mm or 13 mm spacers for LLIF performance [41]. Therefore, it is clear that the anterior column construction representative of ALL plays a key role in stabilization, and this was also demonstrated by these findings using our standard models.

Although many studies have investigated the importance of ALL and factors associated with mechanical complications, there are few reports on the relationship between ALL rupture and instrumentation failure. Recently, a retrospective multicenter study reported that the rate of rod fracture in anterior column realignment (ACR) was 4.4%, although

this rate was not significantly different from that of purposive ALL excision [23] and rod fracture did not occur at the same level, but occurred at the adjacent level of the ALL excision. For this reason, we should also consider the effect of ALL rupture from a biomechanical viewpoint.

Despite significant interest in the ALL and the availability of a number of studies that examined a variety of spinal trials, analysis of the simple effect of ALL rupture using a 3D-FEM, in which the ALL has been modeled and assessed as a solid element, has not been previously performed. Most 3D-FEM studies with posterior fixation models have investigated the effect of differences in surgical approaches, interbody cages, and means of fixation. However, in these studies, ligaments, including the ALL, have always been assessed as bar elements or as tension-only truss or spring elements and were never modeled into solid elements [27, 35, 42, 43]. Therefore, it has not been possible to evaluate the pure effect of the degree of ALL rupture. Our study generated three-dimensional ligaments that were converted into solid elements and we succeeded in dividing the ALL into four fragments. This allowed us to imitate ALL ruptures in 25% increments and examine the association between the degree of ALL rupture and instrumentation failure from a biomechanical perspective.

The present study showed that the stress on the peripheral tissues and the posterior instrument with or without disc excision increased not only at the same level but also at adjacent levels, as the degree of ALL rupture increased. In terms of biomechanics, this result may support the findings of an earlier retrospective multicenter study on rod fractures, although without statistical significance [23]. Moreover, slight displacement occurred regardless of rigid posterior fixation with an increase in the degree of ALL rupture. This may be clinically plausible, and an acquired segmental lordotic angle of about 26° (mean) resulting from accidental ALL rupture in LLIF has been reported [22], which is comparable to the findings reported by studies that assessed the use of hyperlordotic cages under ACR surgery [3, 24, 44]. Therefore, we suggest that ALL rupture is associated with a potential risk of vertebral instability, leading to instrumentation failure. This study does not deny the necessity of ALL excision to correct global alignment, but it does indicate that surgeons should be careful to avoid accidental ALL damage during surgery. We only considered factors affecting ALL rupture, and further investigations into the risk factors for mechanical complications are required.

This study had several limitations. First, the investigated models did not follow the real surgical procedure for ASD and did not involve cage insertion in the IVD space. Assuming that the cage was integrated with a bony union of the adjacent vertebral bodies with the true procedure, the stress on the tissues and posterior instrument may be different in this study; however, this design was necessary to achieve simple and clear analyses. Second, these models imitated a relatively healthy status and did not replicate the degenerative condition found in elderly patients. Third, we did not define the capsular ligament of the facet joint, supraspinous ligament, interspinous ligament, and intertransverse ligament. However, this may not have markedly affected

the present findings because rigid posterior fixation can impede the motion of ligaments and facet joints. Fourth, displacement was the only extension investigated; therefore, it remains unclear what motions (flexion, extension, lateral bending, or axial rotation) are most related to instrumentation failure. Furthermore, we were not able to consider screw loosening because we conducted this experiment under "adhesive" analysis, not "contact" analysis. Despite these limitations, we were able to elucidate the biomechanical relationship between ALL rupture and instrumentation failure.

In conclusion, the stress on the IVDs, vertebral bodies around the screws, and posterior instruments, as well as the displacement during extension, increased as the degree of ALL rupture increased. ALL rupture may cause vertebral instability and create a potential risk of instrumentation failure; therefore, surgeons should be careful to avoid accidental ALL damage during surgery for ASD. A follow-up study evaluating the performance of the model presented in this paper applied to the thoracolumbar spine will be performed in due course.

Acknowledgement

We thank Norihiro Nishida, Masahiro Funaba, Hidenori Suzuki, Yasuaki Imajo and Takashi Sakai, department of orthopedic surgery, Yamaguchi university graduate school of medicine, for their helpful advise on this study. We also thank Rei Kitazumi, Yuto Yamamura and Xian Chen, faculty of engineering, Yamaguchi university, for educating study method. Furthermore, we appreciate kindness of Noriko Minamisono of San-poplar Hospital in Ube city, Yamaguchi prefecture, for creating a supportive work environment.

Conflict of interest: The authors have no conflict of interest to declare.

References

1) **Glassman SD, Bridwell K, Dimar JR, et al.**: The impact of positive sagittal balance in adult spinal deformity. Spine (Phila Pa 1976) **30**, 2024–2029, 2005.
2) **Bess S, Line B, Fu KM, et al.**: The health impact of symptomatic adult spinal deformity: comparison of deformity types to United States population norms and chronic disease. Spine (Phila Pa 1976) **41**, 224–233, 2016.
3) **Saigal R, Mundis GM Jr, Eastlack R, et al.**: Anterior column realignment (ACR) in adult spinal deformity correction: technique and review of the literature. Spine (Phila Pa 1976) **41**, S66–S73, 2016.
4) **Cloyd JM, Acosta FL Jr, Cloyd C, et al.**: Effects of age on perioperative complications of extensive multilevel thoracolumbar spinal fusion surgery. J Neurosurg Spine **12**, 402–408, 2010.
5) **Woods KRM, Billys JB** and **Hynes RA**: Technical description of oblique lateral interbody fusion at L1-L5 (OLIF25) and at L5-S1 (OLIF51) and evaluation of complication and fusion rates. Spine J **17**, 545–553, 2017.
6) **Oliveira L, Marchi L, Coutinho E, et al.**: A radiographic assessment of the ability of the extreme lateral interbody fusion procedure to indirectly decompress the neural elements. Spine (Phila Pa 1976) **35**, S331–S337, 2010.
7) **Kepler CK, Sharma AK, Huang RC, et al.**: Indirect foraminal decompression after lateral transpsoas interbody fusion. J Neurosurg Spine **16**, 329–333, 2012.
8) **Malham GM, Parker RM, Goss B, et al.**: Clinical results and limitations of indirect decompression in spinal stenosis with laterally implanted interbody cages: results from a prospective cohort study. Eur Spine J **24**, S339–S345, 2015.
9) **Castellvi AE, Nienke TW, Marulanda GA, et al.**: Indirect decompression of lumbar stenosis with transpsoas interbody cages and percutaneous posterior instrumentation. Clin Orthop Relat Res **472**, 1784–1791, 2014.

10) **Park P, Wang MY, Lafage V, et al.**: Comparison of two minimally invasive surgery strategies to treat adult spinal deformity. J Neurosurg Spine **22**, 374–380, 2015.
11) **Ozgur BM, Aryan HE, Pimenta L, et al.**: Extreme lateral interbody fusion (XLIF): a novel surgical technique for anterior lumbar interbody fusion. Spine J **6,** 435–443, 2006.
12) **Silvestre C, Mac-Thiong J-M, Hilmi R, et al.**: Complications and morbidities of mini-open anterior retroperitoneal lumbar interbody fusion: oblique lumbar interbody fusion in 179 patients. Asian Spine J **6**, 89–97, 2012.
13) **Fujibayashi S, Hynes RA, Otsuki B, et al.**: Effect of indirect neural decompression through oblique lateral interbody fusion for degenerative lumbar disease. Spine (Phila Pa 1976) **40**, E175–E182, 2015.
14) **Ohtori S, Mannoji C, Orita S, et al.**: Mini-open anterior retroperitoneal lumbar interbody fusion: oblique lateral interbody fusion for degenerated lumbar spinal kyphoscoliosis. Asian Spine J **9**, 565–572, 2015.
15) **Smith JS, Klineberg E, Lafage V, et al.**: Prospective multicenter assessment of perioperative and minimum 2-year postoperative complication rates associated with adult spinal deformity surgery. J Neurosurg Spine **25**, 1–14, 2016.
16) **Auerbach JD, Lenke LG, Bridwell KH, et al.**: Major complications and comparison between 3-column osteotomy techniques in 105 consecutive spinal deformity procedures. Spine (Phila Pa 1976) **37**, 1198–1210, 2012.
17) **Murray G, Beckman J, Bach K, et al.**: Complications and neurological deficits following minimally invasive anterior column release for adult spinal deformity: a retrospective study. Eur Spine J **24**, S397–S404, 2015.
18) **Sugawara R, Takeshita K, Inomata Y, et al.**: The Japanese Scoliosis Society Morbidity and Mortality survey in 2014: The complication trends of spinal deformity surgery from 2012 to 2014. Spine Surg Relat Res **3**, 214–221, 2019.
19) **Wang H, Guo J, Wang S, et al.**: Instrumentation failure after posterior vertebral column resection in adult spinal deformity. Spine (Phila Pa 1976) **42**, 471–478, 2017.
20) **Fujibayashi S, Kawakami N, Asazuma T, et al.**: Complications associated with lateral interbody fusion: nationwide survey of 2998 cases during the first 2 years of its use in Japan. Spine (Phila Pa 1976) **42**, 1478–1484, 2017.
21) **Joseph JR, Smith BW, La Marca, et al.**: Comparison of complication rates of minimally invasive transforaminal lumbar interbody fusion and lateral lumbar interbody fusion: a systematic review of the literature. Neurosurg Focus **39**, E4, 2015.
22) **Nakashima H, Kanemura T, Satake K, et al.**: Factors affecting postoperative sagittal alignment after lateral lumbar interbody fusion in adult spinal deformity: posterior osteotomy, anterior longitudinal ligament rupture, and endplate injury. Asian Spine J **13**, 738–745, 2019.
23) **Godzik J, Haglin JM, Alan N, et al.**: Retrospective multicenter assessment of rod fracture after anterior column realignment in minimally invasive adult spinal deformity correction. World Neurosurg **130**, e400–e405, 2019.
24) **Hosseini P, Mundis GM Jr, Eastlack RK, et al.**: Preliminary results of anterior lumbar interbody fusion, anterior column realignment for the treatment of sagittal malalignment. Neurosurg Focus **43**, E6, 2017.
25) **Cheung ZB, Chen DH, White SJW, et al.**: Anterior column realignment in adult spinal deformity: a case report and review of the literature. World Neurosurg **123**, e379–e386, 2019.
26) **Tatsuno R, Ebata S, Ohba T, et al.**: The preoperative predictions and postoperative fusion rate at the disc level of anterior longitudinal ligament rupture after lateral interbody fusion. J Spine Res **8**, 1640–1645, 2017.
27) **Lee CH, Kim YE, Lee HJ, et al.**: Biomechanical effects of hybrid stabilization on the risk of proximal adjacent-segment degeneration following lumbar spinal fusion using an interspinous device or a pedicle screw-based dynamic fixator. J Neurosurg Spine **27**, 643–649, 2017.
28) **Zhang ZJ, Li H, Fogel GR, et al.**: Finite element model predicts the biomechanical performance of transforaminal lumbar interbody fusion with various porous additive manufactured cages. Comput Biol Med **95**, 167–174, 2018.
29) **Nishida N, Ohgi J, Jiang F, et al.**: Finite element method analysis of compression fractures on whole-spine models including the rib cage. Comput Math Methods Med **5**, 8348631, 2019.
30) **Mattucci SFE, Moulton JA, Chandrashekar N, et al.**: Strain rate dependent properties of younger human cervical spine ligaments. J Mech BehavBiomech Mat **10**, 216–226, 2012.

31) **Ottardi C, Galbusera F, Lucac A, et al.**: Finite element analysis of the lumbar destabilization following pedicle subtraction osteotomy. Med Eng Phys **38**, 506–509, 2016.
32) **Galbusera F, Bellini C, Anasetti F, et al.**: Rigid and flexible spinal stabilization devices: a biomechanical comparison. Med Eng Phys **33**, 490–496, 2011.
33) **Patwardhan AG, Havey RM, Meade KP, et al.**: A follower load increases the load-carrying capacity of the lumbar spine in compression. Spine (Phila Pa 1976) **24**, 1003–1009, 1999.
34) **Renner SM, Natarajan RN, Patwardhan AG, et al.**: Novel model to analyze the effect of a large compressive follower pre-load on range of motions in a lumbar spine. J Biomech **40**, 1326–1332, 2007.
35) **Fan W** and **Guo L-X**: A comparison of the influence of three different lumbar interbody fusion approaches on stress in the pedicle screw fixation system: Finite element static and vibration analyses. Int J Numer Method Biomed Eng **35**, e3162, 2019.
36) **White A** and **Panjabi M**: Clinical biomechanics of the spine, 2nd ed, pp. 21-22, J.B. Lippincott Company, Philadelphia, 2001.
37) **Rundell SA, Auerbach JD, Balderston RA, et al.**: Total disc replacement positioning affects facet contact forces and vertebral body strains. Spine (Phila Pa 1976) **33**, 2510 –2517, 2008.
38) **Denozière G** and **Ku DN**: Biomechanical comparison between fusion of two vertebrae and implantation of an artificial intervertebral disc. J Biomech **39**, 766–775, 2006.
39) **Marchi L, Oliveira L, Coutinho E, et al.**: The importance of the anterior longitudinal ligament in lumbar disc arthroplasty: 36-Month follow-up experience in extreme lateral total disc replacement. Int J Spine Surg **6**, 18–23, 2012.
40) **Sun X, Wang J, Liu X, et al.**: Degeneration of injured intervertebral discs affected by anterior longitudinal ligament injury in rabbits. Int J Clin Exp Pathol **11**, 595–603, 2018.
41) **Kim C, Harris JA, Muzumdar A, et al.**: The effect of anterior longitudinal ligament resection on lordosis correction during minimally invasive lateral lumbar interbody fusion: Biomechanical and radiographic feasibility of an integrated spacer/plate interbody reconstruction device. Clin Biomech (Bristol, Avon) **43**, 102–108, 2017.
42) **Lee CH, Kim YE, Lee HJ, et al.**: Biomechanical effects of hybrid stabilization on the risk of proximal adjacent-segment degeneration following lumbar spinal fusion using an interspinous device or a pedicle screw–based dynamic fixator. J Neurosurg Spine **27**, 643–649, 2017.
43) **Vadapalli S, Sairyo K, Goel VK, et al.**: Biomechanical rationale for using polyether-etherketone (PEEK) spacers for lumbar interbody fusion–a finite element study. Spine (Phila Pa 1976) **31**, E992–E998, 2006.
44) **Januszewski J, Beckman JM, Harris JE, et al.**: Biomechanical study of rod stress after pedicle subtraction osteotomy versus anterior column reconstruction: a finite element study. Surg Neurol Int **8**, 207, 2017.

岩手医誌 74 巻，2 号（令和 4 年 6 月）47-59 頁.

初期器械固定における腰椎前縦靭帯損傷の影響：3 次元有限要素法による研究

楊　寛隆，遠藤寛興，
山部大輔，千葉佑介，及川諒介，
村上秀樹，土井田稔

岩手医科大学医学部，整形外科学講座

(Received on December 28, 2021 & Accepted on February 5, 2022)

要旨

成人脊柱変形に対して側方進入腰椎椎体間固定術を併用した手術による術中合併症の一つとして腰椎前縦靭帯 (anterior longitudinal ligament；ALL) 損傷があり，近年，これに伴う術後 instrumentation failure 症例が報告されている．3 次元有限要素法を用いて ALL 損傷による instrument への影響を検討した．CT 画像から 3 次元有限要素法腰椎モデルを作成し，至適に instrument を設置された L1-S1 固定モデルも作成した．これらに対して実際の手術手技のように L3/4 高位で椎間板部分切除を模擬し，同高位で ALL を 25% ずつ損傷させたモデルとした．これらの伸展方向への変位量 (mm) と椎間板，スクリュー周囲の椎体，instrument へのかかる von Mises 応力 (MPa) を評価した．ALL 損傷率が上昇するほど伸展方向への変位量が増加した．同様に椎間板，スクリュー周囲の椎体，instrument への応力が上昇した．また instrument への応力は損傷高位と隣接する高位においても上昇した．ALL 損傷の程度が増加するほど脊椎不安定性が生じ組織と instrument への負荷が上昇した．ALL 損傷は術後 instrumentation failure のリスクとなり得る．